Neurosci. Bull. December, 2020, 36(12):1484–1499
https://doi.org/10.1007/s12264-020-00594-4

www.neurosci.cn
www.springer.com/12264

ORIGINAL ARTICLE

Connexin 36 Mediates Orofacial Pain Hypersensitivity Through GluK2 and TRPA1

Qian Li[1] · Tian-Le Ma[1] · You-Qi Qiu[1] · Wen-Qiang Cui[1,2] · Teng Chen[1] · Wen-Wen Zhang[1] · Jing Wang[3] · Qi-Liang Mao-Ying[1] · Wen-Li Mi[1] · Yan-Qing Wang[1] · Yu-Xia Chu[1]

Received: 25 March 2020 / Accepted: 6 September 2020 / Published online: 16 October 2020

Abstract Trigeminal neuralgia is a debilitating condition, and the pain easily spreads to other parts of the face. Here, we established a mouse model of partial transection of the infraorbital nerve (pT-ION) and found that the Connexin 36 (Cx36) inhibitor mefloquine caused greater alleviation of pT-ION-induced cold allodynia compared to the reduction of mechanical allodynia. Mefloquine reversed the pT-ION-induced upregulation of Cx36, glutamate receptor ionotropic kainate 2 (GluK2), transient receptor potential ankyrin 1 (TRPA1), and phosphorylated extracellular signal regulated kinase (p-ERK) in the trigeminal ganglion. Cold allodynia but not mechanical allodynia induced by pT-ION or by virus-mediated overexpression of Cx36 in the trigeminal ganglion was reversed by the GluK2 antagonist NS102, and knocking down Cx36 expression in Nav1.8-expressing nociceptors by injecting virus into the orofacial skin area of Nav1.8-Cre mice attenuated cold allodynia but not mechanical allodynia. In conclusion, we show that Cx36 contributes greatly to the development of orofacial pain hypersensitivity through GluK2, TRPA1, and p-ERK signaling.

Keywords Orofacial pain · Gap junction · Glutamate receptor ionotropic kainate 2 · Transient receptor potential A1

Introduction

Trigeminal nerve injury causes persistent orofacial neuropathic pain, and one of the prominent features of such injury is ectopic pain [1, 2]. Ectopic pain refers to the spread of pain from the area innervated by the injured nerve to the area innervated by the intact nerve [3]. The induction of trigeminal neuropathic pain, especially ectopic pain, seriously affects the quality of life in patients. The underlying mechanisms behind such pain remain unclear, but it has been proposed that primary sensory neurons become activated and sensitized following trigeminal nerve injury [4, 5] and that intact neurons and satellite glial cells (SGCs) then also become sensitized through nitric oxide released by the injured neurons [3] and through mutual information transmission between neurons in the trigeminal ganglion (TG) *via* calcitonin gene-related peptide (CGRP) [6] and various molecules such as Ca^{2+} and glutamate [7]. Therefore, the direct or indirect activation of adjacent neurons or SGCs by the injured cells might contribute greatly to the induction of ectopic orofacial pain.

Gap junctions (also known as electrical synapses) allow electrical signals and small cytoplasmic molecules that are no more than 1 kDa in size to pass quickly between cells [8]. Allodynia can be explained by the "ignition theory"

Qian Li, Tian-Le Ma and You-Qi Qiu contributed equally to this work.

Electronic supplementary material The online version of this article (https://doi.org/10.1007/s12264-020-00594-4) contains supplementary material, which is available to authorized users.

✉ Yu-Xia Chu
yuxiachu@fudan.edu.cn

1 Department of Integrative Medicine and Neurobiology, Institutes of Integrative Medicine, School of Basic Medical Sciences, Institutes of Brain Science, Brain Science Collaborative Innovation Center, State Key Laboratory of Medical Neurobiology, and MOE Frontiers Center for Brain Science, Fudan University, Shanghai 200031, China

2 Department of Pain Management, Shandong Provincial Qianfoshan Hospital, The First Hospital Affiliated with Shandong First Medical University, Jinan 250000, China

3 Department of Nephropathy, The Third Affiliated Hospital of Shenzhen University, Luohu Hospital Group, Shenzhen 518001, China

[9] in which the electrical communication depends on the transmission of chemicals between neurons [10, 11], and thus gap junctions might play a role in allodynia. Gap junctions are made up of connexins (Cxs), and among these the relationship between Cx43 and pain has been widely reported. Cx43 is distributed among SGCs, and contributes to the activation of glial cells [12, 13]. Peripheral nerve injury causes increased expression of Cx43 [14, 15], and blockade of Cx43 [16] or RNA interference of the *Gja1* gene [17] attenuates allodynia. The gap junctions between SGCs of the TG are mainly composed of Cx43, which plays an important role in the induction of ectopic orofacial pain [18]. In addition to the SGC-SGC coupling formed by Cx43, dual-cell patch clamp recordings have provided evidence of neuron-neuron and neuron-SGC electrical coupling in the TG [19], and the function of such connections in the induction and spread of orofacial pain is worth investigating.

There are at least four kinds of Cxs in the TG that are related to pain and inflammation: Cx36, Cx26, Cx40, and Cx43 [20]. Cx36 is the only subtype that is specifically expressed and widely distributed between neurons [21]. Cx36 contributes to the electrical coupling that plays a critical role in synchronizing rhythmic activity within the olivary nucleus [22], and the electrical synapses formed by Cx36 between intermediate neurons are essential for inhibitory γ oscillation [23]. However, few studies have investigated the function of Cx36 in the development of pain, especially orofacial pain. One report has shown that Cx36 in the medullary dorsal horn contributes greatly to mechanical allodynia through coupling GABAergic neurons [24]. The expression of Cx36 mRNA and protein is detectable in the TG, and Cx36 is distributed in neurons that express substance P, CGRP, and some temperature-sensitive transient receptor potential channels [25] that are closely related to pain production. Moreover, the expression of Cx36 and Cx40 in neurons is increased in animal models of inflammation, but there is no significant increase in Cx43 in astrocytes [26], and our previous study found significant upregulation of Cx36 following partial transection of the infraorbital nerve (pT-ION) [27].

From the above, we hypothesized that upregulated expression of Cx36 plays a vital role in the increased coupling between neurons, which then forms a more highly connected network for rapid signal exchange and thus lays the foundation for primary and secondary allodynia.

We therefore designed experiments to determine whether Cx36 expression would increase after pT-ION, whether functional blockade of Cx36 by the Cx36 inhibitor mefloquine could alleviate pT-ION-induced mechanical and cold allodynia, and whether the increase in the downstream molecules could be reversed. Moreover, we knocked down Cx36 expression using short hairpin RNA (shRNA)-carrying viruses in Nav1.8-Cre transgenic mice to specifically examine the roles of Cx36 and its downstream molecules in Nav1.8-positive neurons in the pT-ION-induced pain-like behaviors.

Materials and Methods

Animals

All experiments conducted in the present work were approved by the Fudan University Institutional Animal Care and Use Committee and were performed according to the ethical standards of the International Association for the Study of Pain. Male C57Bl/6 mice 6–8 weeks of age and were obtained from the Shanghai Laboratory Animal Center of the Chinese Academy of Sciences. The mice were kept under fixed conditions of 23°C and 12 h of light/dark cycling with free access to food and water. A total of 4–8 animals were placed in a cage for acclimation at least 2 weeks before experiments. Nav1.8-Cre mice were a gift from Dr. Qiufu Ma (Harvard University, Boston, USA) with the permission of Dr. John Wood (University College London, London, UK). All surgery was performed under Avertin anesthesia. The experimenters tried their best to reduce the number and suffering of animals used.

pT-ION Surgery

Mice in the pT-ION group were subjected to pT-ION surgery, which has been shown to rapidly induce stable peripheral neuropathy in mice [27]. After anesthesia with Avertin [350 mg/kg, intraperitoneal (*i.p.*), T48402, Sigma-Aldrich, St. Louis, MO], a cavity was exposed in the left palate and the infraorbital nerve under the mucosa was exposed using angled clamps. The deep branch of the infraorbital nerve innervating the ventral edge of the left vibrissal pad and upper lip was tightly bound with 4.0 catgut, and the distal end was cut open to remove a 1 – 2 mm segment of the distal nerve. Tissue glue was used to close the incision. Mice in the sham group were anesthetized and the infraorbital nerve exposed as described above, but without nerve ligation or amputation.

Behavioral Testing

Mechanical Allodynia

The experimenters were blinded to the group assignments in the behavioral tests. The ipsilateral hairs in the V2 and V3 skin areas were removed using a hair clipper (HC1066, Philips, Netherlands) three days before the baseline behavioral tests. Mice were handled and conditioned once

a day for 3 days before the tests. During the tests of mechanical allodynia, the mice were placed on the palm of the experimenter's hand for 3 min of adaptation. When the head was stabilized, a set of von Frey fibers (Stoelting, Wood Dale, IL) were poked into its left face in the V2 and V3 skin areas. The bending force of the von Frey fibers varied from 0.07 to 2.0 g, and each fiber was bent to 90° in order to keep the stimulation consistent. A positive reaction was recorded when the mouse flicked its head quickly in response to a complete stimulation. The skin was stimulated five times with each fiber with 30-s intervals between stimulations. The force (g) of the von Frey fiber with three positive reactions among five stimulations was recorded as the threshold of mechanical allodynia. Mice were allowed to move freely during the whole process of behavioral testing.

Cold Allodynia

When we tried to perform the acetone test in the V2 area during the preliminary experiments, we found that it was difficult to avoid spraying acetone into the eyes, and this severely influenced the subsequent behavioral testing. Therefore, the acetone test was performed only in the V3 area. During the test, each mouse was held gently to keep the head fixed, and a 1 mL syringe (Hamilton, Reynolds, NV) was used to drip 50 μL acetone onto the V3 area of the left side. We tried to protect the eyes by delivering all of the acetone quickly and evenly. Cold hypersensitivity induced by the evaporation of acetone was assessed by the mouse rubbing or grabbing the skin in the V3 region using its front or rear paws. The total duration of wiping caused by the acetone was recorded starting immediately after its application.

Open Field Test

The box for the test was 50 × 50 × 40 cm^3 with a central zone of 25 × 25 cm^2. We put each mouse in the central area and the monitor was started at the same time. The movement of the mouse within the box over the course of 5 min was recorded and calculated using video analysis software (Shanghai Mobile Datum Information Technology Co., Shanghai, China). All of the tests were conducted in a dim and quiet experimental room.

Immunofluorescence Staining

The removal and sectioning of the left TG and immunofluorescence staining were performed as described previously [27]. Briefly, mice were deeply anesthetized using Avertin (350 mg/kg, *i.p.*) and perfused with PBS followed by 4% paraformaldehyde (80096618, Hushi, Shanghai, China). The TG sections were cut at 10 μm on a microtome. The primary antibodies were as follows: mouse anti-Cx36 (1:50, sc398063, Santa Cruz Biotechnology, Dallas, TX), goat anti-CGRP (1:500, ab36001, Abcam, Cambridge, UK), mouse anti-neurofilament 200 (NF-200, 1:50, N5389, Sigma-Aldrich, St. Louis, MO), rabbit anti-TRPA1 (1:200, NB110-40763, Novus Biologicals, Centennial, CO), rabbit anti-GluK2 (1:400, AGC-009, Alomone Labs, Jerusalem, Israel), and mouse anti-Cre (1:1,000, MAB3120, Sigma-Aldrich). The mixed secondary antibodies included Alexa 488-conjugated, Alexa 594-conjugated, and Alexa 647-conjugated IB4 antibodies (1:1,000, Invitrogen, Rockford, IL). The sections were coverslipped with DAPI-Fluoromount-G and observed under a multiphoton laser point scanning confocal microscopy system (FV1000, Olympus, Tokyo, Japan). For each experiment, images were captured using same acquisition parameters, processed simultaneously, and analyzed using ImageJ (version 1.8.0; NIH). For single immunofluorescence, the optical density of immunoreactive (IR) staining for Cx36, GluK2, or TRPA1 was measured. The density of IR for each protein was determined by subtracting the background density, and six sections for each mouse were averaged to provide a mean density of IR (n = 4/group). For double immunofluorescence, if the expression of Cx36 or GluK2 (green) in Nav1.8-positive neurons (Cre, red) increased, the area of the merged signal (yellow) was larger, and thus the area of the yellow signal was used to reflect the co-localization intensity. To compare the co-localization of Cx36 or GluK2 and Cre in different groups, six TG sections (n = 4/group) were randomly selected, analyzed, and averaged to obtain the co-localization intensity.

Western Blotting

The treatment of the left TG samples and the following western blotting procedures were also the same as described in our previous work [27]. In brief, protein samples of the left TG were separated by SDS-PAGE and then transferred onto PVDF membranes, which were then blocked with 5% milk and incubated with primary antibodies at 4°C overnight and then incubated with the HRP-conjugated secondary antibody. Listed below are the primary antibodies used in the incubation: mouse anti-Cx36 (1:100, sc398063, Santa Cruz Biotechnology), rabbit anti-TRPA1 (1:500, NB110-40763, Novus Biologicals, CO, USA), rabbit anti-GluK2 (1:400, AGC-009, Alomone Labs), rabbit anti-ERK and anti-p-ERK (1:2,000, Cell Signaling Technology, Danvers, MA), HRP-conjugated mouse anti-β-actin (1:10,000, 4967, Cell Signaling Technology), and HRP-conjugated rabbit anti-β-tubulin (1:5000, 5346, Cell Signaling Technology). The secondary antibodies were HRP-conjugated goat anti-rabbit IgG

(H+L) (1:10,000, SA00001-2, Proteintech) or HRP-conjugated goat anti-mouse IgG (H+L) (1:10,000, SA00001-1, Proteintech). When necessary, western blot stripping buffer (21059, Thermo Fisher, Waltham, MA) was used to remove the combined primary and secondary antibodies of one protein from the PVDF membrane in order to re-detect the other proteins. The intensities of the bands were quantified using Quantity One analysis software (Version 4.6.2, Bio-Rad Laboratories, Hercules, CA) and normalized against the density of β-actin or tubulin.

Drug Administration

Mefloquine (M2319, Sigma-Aldrich), a specific inhibitor of Cx36 [28], was made up in suspension with Tween-80 and then dissolved and diluted in normal saline. Repeated i.p. injection of mefloquine was performed in each mouse at 20 or 30 mg/kg once a day from day 7 to day 13 after pT-ION. A single *i.p.* injection of the competitive GluK2 antagonist NS102 (N179, Sigma-Aldrich) was applied at 80, 40, or 8 μmol/L in a volume of 0.1 mL per mouse on day 21 after pT-ION and on day 28 after AAV-Cx36-Ove virus injection. NS 102 was prepared as a stock solution in DMSO (D2650, Sigma-Aldrich) and diluted with DMSO at first and further diluted with normal saline before experiments. The concentration of DMSO in the drug solution was 5%.

Adeno-Associated Virus (AAV)-Mediated Gene Knockdown and Overexpression

For the Cx36 knockdown experiment, the vector-mediated miR30-based short hairpin RNA (shRNA) knockdown strategy was used. In detail, for Cre-dependent expression of shRNAs in transgenic mice, the shRNA coding sequence targeting mouse Gjd2 (5-GCAGCACTCCACTATGATT-3) was cloned into the pAAV-CBG-LSL-EGFP-3xFlAG-WPRE vector (OBiO Technology Co., Ltd., Shanghai, China) using the BsrGl/Hindlll restriction sites. AAV2/Retro-CBG-LSL-EGFP-miR30shRNA(Gjd2)-WPRE and its control AAV2/Retro-CBG-LSL-EGFP-3xFlAG-WPRE virus were packaged by OBiO Technology. Gjd2 is the encoding gene of Cx36, and the above gene construction achieved the retrograde and Cre-dependent interference of Gjd2 expression, and thus resulted in the downregulation of Cx36 in TG neurons after subcutaneous virus injection. For the Cx36 overexpression experiment, the coding sequence of mouse Cx36 (NC_000068.7) was designed and packaged as an AAV2/Retro virus (rAAV-CMV-Gjd2-P2A-EGFP-WPRE) by BrainVTA (Hubei, China). The control virus was constructed as rAAV-CMV-EGFP. Mice were deeply anesthetized by Avertin (350 mg/kg, *i.p.*), and 8 μL of virus was injected into four sites in the V2 and V3 areas for the Cx36 knockdown experiment while 6 μL of virus was injected into three sites in the V2 area for the Cx36 overexpression experiment using a 10 μL syringe (Hamilton Co.). The rate of injection was 1 μL/min. The doses of AAV-Cx36-Interfering (AAV-Cx36-Int) virus and AAV-Cx36-Overexpressing (AAV-Cx36-Ove) virus were 3.80×10^{12} viral genomes (v.g.)/mL and 5.60×10^{12} v.g./mL, respectively. After injection into each site, the needle was retained for 1 min.

Statistical Analysis

The data were analyzed by GraphPad Prism 8 (GraphPad Software Inc., San Diego, CA) and are presented as means ± SEM. One-way analysis of variance (ANOVA) followed by Tukey's test or Dunnett's multiple comparisons test and Student's *t*-test were used to compare the differences between two groups. The data from the behavioral tests were analyzed by two-way repeated-measures (RM) ANOVA followed by Sidak' s test or Tukey's test. The linear correlation between data from two groups was analyzed using Pearson's correlation. $P < 0.05$ was adopted as the significance threshold for all analyses.

Results

The Cx36 Inhibitor Mefloquine Ameliorates the pT-ION-induced Primary and Secondary Orofacial Allodynia, Especially Cold Allodynia

We used the pT-ION mouse model of trigeminal neuralgia, which has been used in previous work [27]. This model was established by the ligation and subsequent partial transection of the infraorbital nerve. The V2 skin area was innervated by the injured nerve, and the allodynia in this area is referred to as primary allodynia, while that in the uninjured nerve-innervated V3 area is referred to as secondary allodynia. A lower threshold response upon mechanical stimulation from the von Frey filament compared to baseline or the sham group is defined as mechanical allodynia. From day 7 after the pT-ION surgery, the thresholds in response to von Frey hair stimulation in the V2 and V3 areas ipsilateral to the injured nerve were significantly reduced compared to the sham group and remained stable for the following 21 days (Fig. 1A, B). Cold allodynia in the V3 area was also induced compared to the sham group, with significantly prolonged duration of wiping time caused by acetone starting from day 7 after surgery and lasting for at least 21 days (Fig. 1C).

To ascertain the contribution of Cx36 to neuropathic orofacial allodynia, mice were injected i.p. with mefloquine, an inhibitor of Cx36, on day 7 after pT-ION.

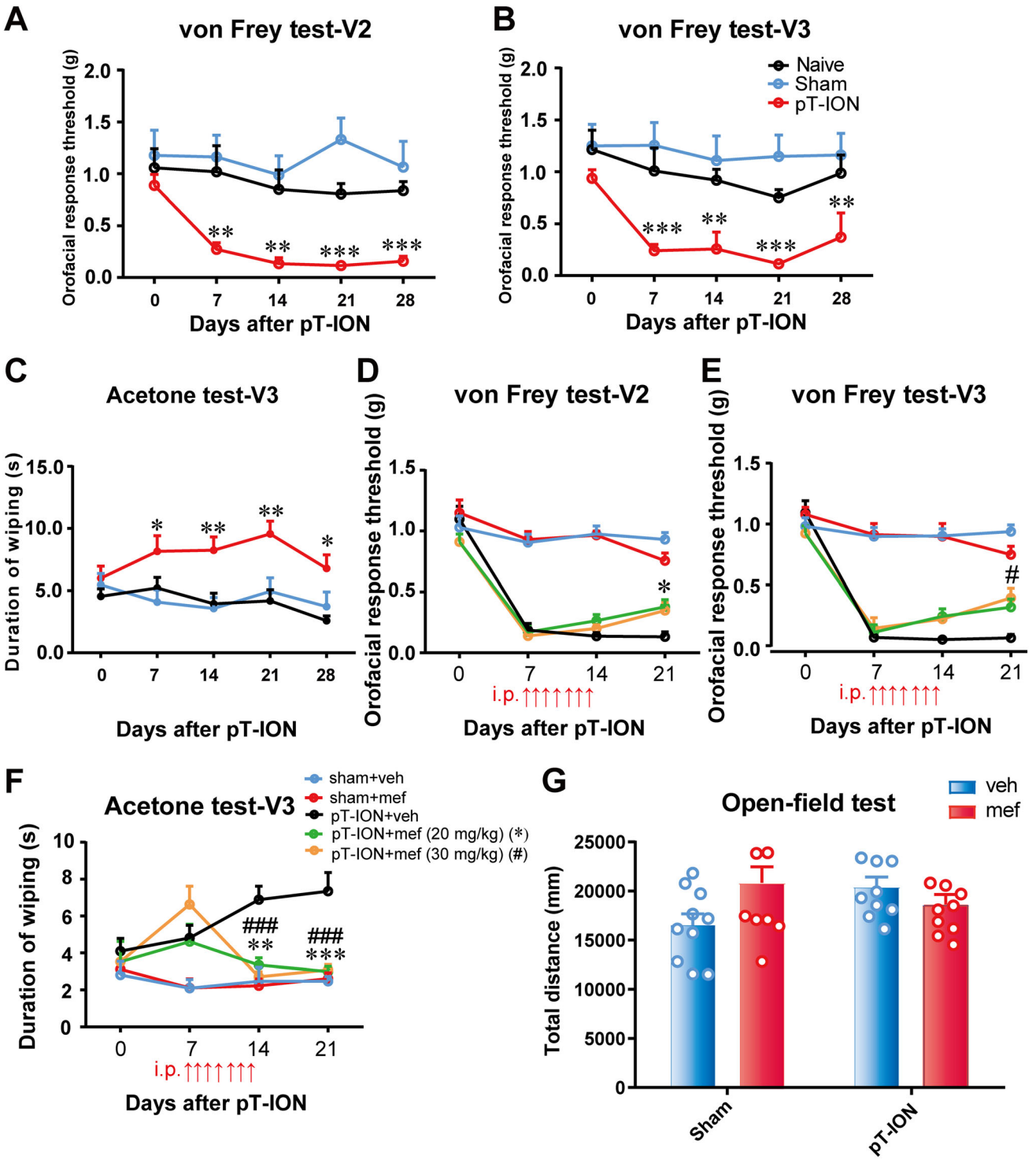

Fig. 1 Pharmacological inhibition of Cx36 reverses pT-ION-induced orofacial allodynia. **A**–**C** pT-ION leads to long-lasting primary (**A**) and secondary (**B**) mechanical allodynia in the ipsilateral V2 and V3 areas and to secondary cold allodynia (**C**) in the ipsilateral V3 area. Data are shown as means ± SEM, n = 8/group. $^{*}P < 0.05$, $^{**}P < 0.01$, and $^{***}P < 0.001$ *vs* sham group (two-way RM ANOVA followed by Tukey's test). **D**–**F** Mefloquine (mef) at two doses for 7 consecutive days, significantly suppresses pT-ION-induced primary (**D**) and secondary (**E**) mechanical allodynia and secondary cold allodynia (**F**) in the V2 and V3 areas (arrows, time points of mefloquine injection). Data are shown as means ± SEM, n = 10/group. $^{*}P < 0.05$, $^{**}P < 0.01$, and $^{***}P < 0.001$, pT-ION+mef (20 mg/kg) *vs* pT-ION+veh; $^{\#}P < 0.05$ and $^{\#\#\#}P < 0.001$, pT-ION+mef (30 mg/kg) *vs* pT-ION+veh (two-way RM ANOVA followed by Tukey's test). **G** The open-field test shows no difference in total distance among the four groups at 20 mg/kg mefloquine (n = 10; two-way ANOVA followed by Sidak's test).

Because stable primary and secondary orofacial allodynia was established on day 7 after pT-ION, the effects of mefloquine on established allodynia were evaluated at that time point. The mefloquine was administered at either 20 or 30 mg/kg daily for 7 days. Compared to the pT-ION+veh group, both doses of mefloquine significantly reversed the mechanical allodynia in the V2 and V3 regions, and the effect was similar for both doses (Fig. 1D, E). It should be noted that while mefloquine only partially rescued the mechanical allodynia, it completely reversed the pT-ION-induced cold allodynia (Fig. 1F), which indicated that Cx36 is more involved in trigeminal nerve injury-induced cold pain. To test whether mefloquine had an effect on motor function, the open-field test was performed on day 21 after pT-ION. The total distance was measured and showed no significant difference when mefloquine was applied at 20 mg/kg in pT-ION mice (Fig. 1G). However, we found that the higher dose of mefloquine at 30 mg/kg resulted in movement deficiency (data not shown), so 20 mg/kg was chosen as the treatment dose in the subsequent experiments. In addition, mefloquine had no significant impact on movement in the sham groups (Fig. 1G).

Trigeminal Nerve Injury Induces Increased Cx36 Expression in the TG

Immunofluorescence staining images of Cx36 in the TG are shown in Fig. 2A. We measured the expression of Cx36 in the TG on days 1, 3, 5, 7, 14, 21, and 28 after pT-ION surgery. The level of Cx36 increased significantly from day 5 and lasted up to 28 days (Fig. 2B, C). If aberrant Cx36 expression really induces and mediates the primary and secondary orofacial allodynia in mice with trigeminal nerve injury, then changes in Cx36 expression in the ipsilateral TG should be correlated with the occurrence of orofacial allodynia behaviors. Linear regression analysis showed that the level of Cx36 expression in the ipsilateral TG was negatively correlated with the mechanical response thresholds in both the V2 and V3 areas (V2: $P = 0.1248$, $r = -0.7736$, $Y = -1.250*X + 1.683$; V3: $P = 0.0311$, $r = -0.9117$, $Y = -1.493*X + 1.864$; Fig. 2D, E) and was positively correlated with the duration of the wiping response to acetone in the V3 region ($P = 0.0476$, $r = 0.8823$, $Y = 0.3455 * X - 1.248$; Fig. 2F). The relationship between Cx36 upregulation in the TG and orofacial allodynia after pT-ION surgery suggested that Cx36 is critical in inducing orofacial allodynia.

We next determined the distribution of Cx36 in the TG-V2 and TG-V3 neurons of the pT-ION mice (Supplementary Fig. S1A). The TG mainly includes three types of neurons: peptidergic nociceptors (expressing the marker CGRP), non-peptidergic nociceptors (expressing the marker IB4), and large non-nociceptive neurons (expressing the marker NF200). Immunofluorescence staining showed that Cx36 was co-localized with CGRP (Fig. S1B), IB4 (Fig. S1C), and NF200 (Fig. S1D) in both TG-V2 and TG-V3 at 21 days after pT-ION. These results demonstrated that Cx36 is widely distributed in the TG but is not selectively expressed in nociceptors. Moreover, the pT-ION-induced increase in Cx36 expression was observed in both TG-V2 and TG-V3 neurons (Fig. S2), which provided anatomical support for the Cx36-mediated spread of pain.

The Cold Sensor GluK2 is a Potential Downstream Effector of Cx36 in Mediating pT-ION-induced Cold Allodynia

Given the significant alleviation of cold allodynia by mefloquine, we hypothesized that Cx36 blockade changes the expression or function of a cold sensor. A recent study showed that mouse GluK2 in peripheral sensory neurons is involved in mediating cold sensation [29], so we next determined whether GluK2 acts downstream of Cx36 in mediating pT-ION-induced cold allodynia. Immunofluorescence staining showed that GluK2 was expressed in both TG-V2 and TG-V3 neurons after pT-ION (Fig. 3A). GluK2 was upregulated in the ipsilateral TG starting from 7 days to at least 21 days after nerve injury (Fig. 3B). Moreover, the pT-ION-induced upregulation of GluK2 was positively correlated with the increased expression of Cx36 ($P = 0.0443$, $r = 0.9557$, $Y = 0.3781 * X + 0.4898$; Fig. 3C). Immunofluorescence staining also showed a pT-ION-induced increase in GluK2 expression in TG neurons (Supplementary Fig. S2)

To determine the role of GluK2 in mediating primary and secondary allodynia, NS 102, an antagonist of GluK2, was injected on day 21 after pT-ION. NS 102 was tested at 8, 40, and 80 μmol/L in 0.1 mL was injected *i.p.*. The von Frey test and acetone test were carried out at 1, 2, 4, and 24 h after NS 102 injection. We found that blocking GluK2 with NS 102 did not reduce mechanical allodynia in the V2 or V3 areas regardless of the dose or time point (Fig. 4A, B). However, as is shown in Fig 4C, all three doses of NS 102 significantly reversed cold allodynia in the V3 area at 1 and 2 h after drug application. Western blotting showed that NS 102 caused a dose-dependent reduction in the phosphorylation of ERK at 2 h after NS 102 administration (Fig. 4D–F), which is critical in mediating the development of pain [30]. However, no difference in total ERK was shown in response to NS 102. The highest dose, 80 μmol/L, was used in the subsequent experiments. Therefore, the above results demonstrate that GluK2 contributes greatly to cold allodynia, but not mechanical allodynia, perhaps through downstream ERK activation.

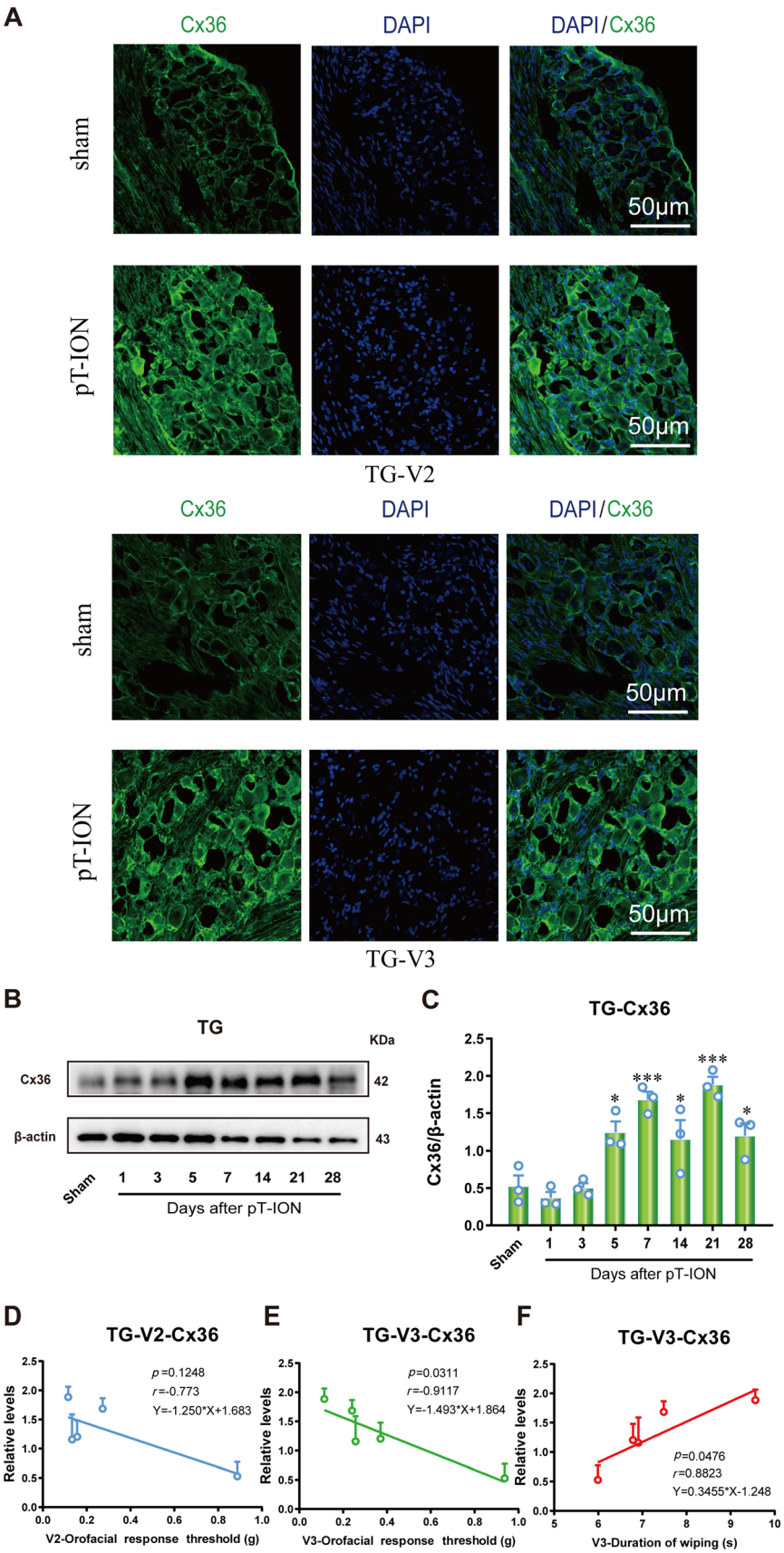

Fig. 2 pT-ION induces upregulation of Cx36 in the TG. **A** Representative images of immunofluorescence staining of Cx36 in the TG on day 14 after surgery. **B**, **C** Time course of Cx36 expression in the ipsilateral TG after pT-ION. Data are shown as means ± SEM, $n = 3$/group. $^{*}P < 0.05$ and $^{***}P < 0.001$ *vs* sham (one-way ANOVA followed by Dunnett's test). **D–F**, Linear correlation between Cx36 expression and orofacial response threshold (g) in the V2 and V3 and duration of wiping (s). (**D**: $P = 0.1248$, $r = -0.7736$; **E**: $P = 0.0311$, $r = -0.9117$; **F**: $P = 0.0476$, $r = 0.8823$).

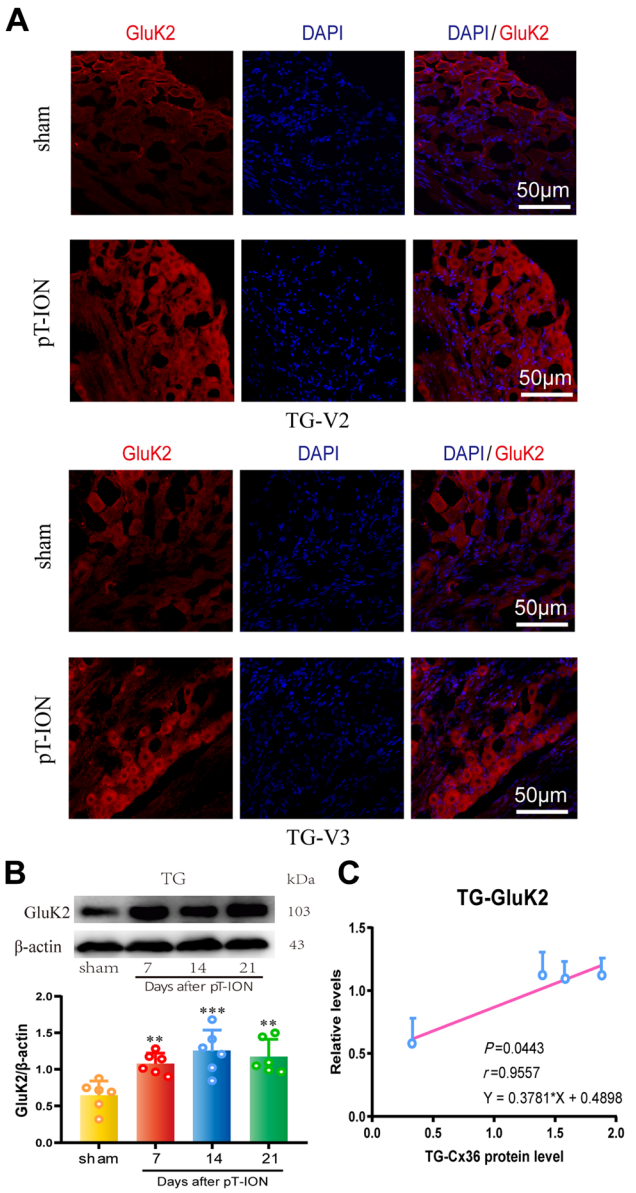

Fig. 3 pT-ION induces upregulation of GluK2. **A** Representative images of immunofluorescence staining of GluK2 in the TG. DAPI was used to stain the cell nuclei. **B** Time course of GluK2 expression in the ipsilateral TG after pT-ION (TGs from the sham group were obtained on day 7 after surgery). Data are shown as means ± SEM, $n = 6$/group. $^{**}P < 0.01$ and $^{***}P < 0.001$ *vs* sham (one-way ANOVA analysis followed by Tukey's test). **C** pT-ION-induced increase in GluK2 expression is positively correlated with Cx36 expression in the ipsilateral TG ($P = 0.0443$, $r = 0.9557$).

The Cx36 Inhibitor Mefloquine Reverses the pT-ION-induced Upregulation of TRPA1 in Addition to GluK2 and p-ERK

Because Cx36 blockade alleviated not only cold allodynia, but also the mechanical allodynia induced by PT-ION, and because Cx36 overexpression induced both cold and mechanical allodynia, other molecules downstream of Cx36 may mediate the induction of mechanical allodynia. Given that our previous study showed that the TRPA1 antagonist HC-030031 reverses pT-ION-induced mechanical and cold allodynia [27], TRPA1 might be this downstream molecule. Immunofluorescence staining showed that TRPA1 was co-localized with Cx36 in both the TG-V2 and TG-V3 neurons of pT-ION mice (Fig. 5A, B), and immunofluorescence staining showed a pT-ION-induced increase in TRPA1 expression in the TG-V2 and TG-V3 neurons (Fig. S2). Western blotting showed that pT-ION induced an increase in TRPA1 expression in the TG, and this increase was significantly reversed by repeated application of mefloquine at 20 mg/kg (daily from 7 to 13 days after pT-ION) at day 21 after pT-ION (Fig. 5C, F). Moreover, linear regression analysis showed that the downregulation of TRPA1 due to Cx36 blockade was positively correlated with the decreased expression of Cx36 protein (TRPA1-Cx36: $P = 0.0104$, $r = 0.8319$, $Y = 1.102 * X + 0.01795$, Fig. 5J). In addition, the pT-ION-induced upregulation of GluK2 and p-ERK was also significantly reversed by repeated application of mefloquine, and the downregulation of both GluK2 and p-ERK was positively correlated with the decrease in Cx36 expression following mefloquine application (GluK2-Cx36: $P = 0.0208$, $r = 0.7856$, $Y = 1.198 * X + 0.1418$; p-ERK-Cx36: $P = 0.0334$, $r = 0.7463$, $Y = 0.9241 * X + 0.3188$) (Fig. 5C–E, G–J). No significant differences were seen after mefloquine treatment in mice from the sham groups. These results support the hypothesis that, in addition to GluK2, TRPA1 serves as another downstream effector of Cx36 in mediating trigeminal nerve injury-induced mechanical and cold allodynia.

The Cold Allodynia, but not the Mechanical Allodynia Induced by AAV-mediated Cx36 Overexpression is Reversed by the GluK2 Antagonist NS 102

To demonstrate whether upregulation of Cx36 in the V2 area is sufficient to induce orofacial allodynia, we induced AAV-mediated Cx36 overexpression in the TG-V2 neurons of naïve mice by injecting the virus subcutaneously. The AAV-Cx36-Ove virus or AAV-control virus was subcutaneously injected into three sites in the V2 skin area (Fig. 6A), and 2 μL of virus was injected into each site. This viral vector is retrogradely transported from the nerve endings to the somata and overexpress Cx36 specifically in TG-V2 neurons. This method allowed the virus to specifically target TG-V2 or TG-V3 neurons without infecting neurons in the adjacent TG areas (Fig. S3). The von Frey test and acetone test were carried out every week after viral injection, and the orofacial response thresholds of the ipsilateral V2 and V3 areas were significantly decreased 3

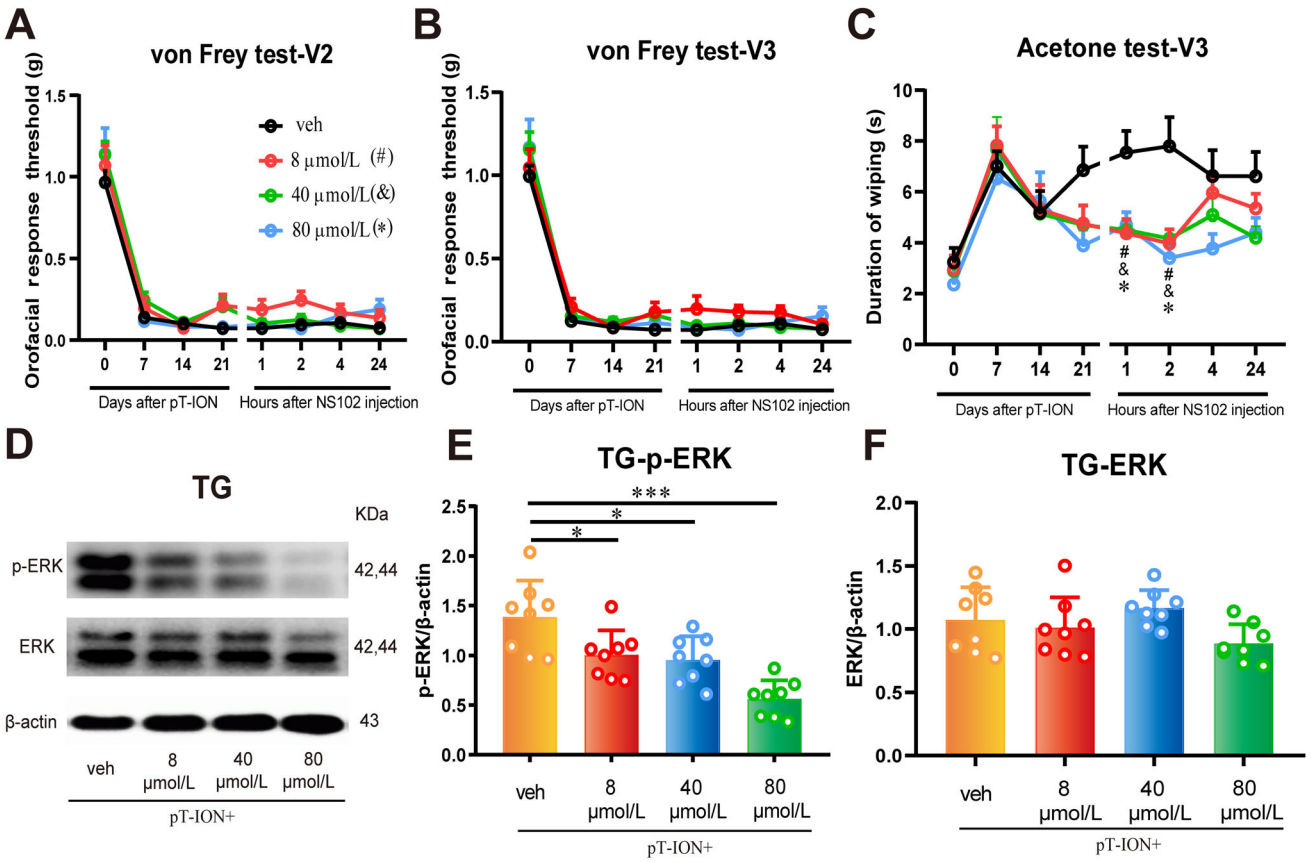

Fig. 4 The GluK2 antagonist NS 102 reverses pT-ION-induced cold allodynia and ERK activation but not mechanical allodynia. **A–C** At day 21 after pT-ION, *i.p.* injection of NS 102 at three doses attenuated cold allodynia in the V3 area (**C**), but not mechanical allodynia in either the V2 (**A**) or V3 (**B**) area at 1 or 2 h after injection. Data are shown as means ± SEM, n = 10/group. #$P < 0.05$ (8 μmol/L), & $P < 0.05$ (40 μmol/L), and *$P < 0.05$ (80 μmol/L) *vs* vehicle (veh) (two-way RM ANOVA followed by Tukey's test). **D–F** Activation of ERK in the ipsilateral TG is reversed by all three doses of NS 102 at 2 h after injection. Data are shown as means ± SEM, n = 10/group. *$P < 0.05$ and ***$P < 0.001$ *vs* veh (one-way ANOVA followed by Tukey's test).

weeks after injection of AAV-Cx36-Ove virus (Fig. 6B, C), and this effect lasted until the final day of the experiment (28 days after virus injection). At the same time, the duration of wiping increased significantly on day 28 after virus injection (Fig. 6D). NS 102 was administered to the mice on day 28 to see whether GluK2 blockade could rescue Cx36 overexpression-induced orofacial allodynia, and we found that the Cx36 overexpression-induced increase in the duration of wiping was significantly reversed (Fig. 6D). However, Cx36 overexpression-induced mechanical allodynia in the V2 and V3 regions was not affected (Fig. 6B, C). Western blots showed that overexpressing Cx36 in the TG-V2 neurons of naïve mice significantly enhanced the expression of GluK2, TRPA1, and p-ERK in the TG ipsilateral to the injury (Fig. 6E–K), and these increases were positively correlated with the upregulation of Cx36 (Fig. 6L). Moreover, the Cx36 overexpression-induced increase in p-ERK expression was reversed by the GluK2 antagonist NS 102 (Fig. 6I, J). These results suggested that upregulation of Cx36 overexpression is sufficient to induce both cold and mechanical allodynia and that GluK2, TRPA1, and p-ERK serve as the downstream effectors of Cx36 in mediating the induction of cold allodynia but not mechanical allodynia.

Selective Knockdown of Cx36 in Nav1.8-expressing Nociceptors Reverses pT-ION-induced Cold Allodynia but not Mechanical Allodynia

It has been proposed that Nav1.8-expressing nociceptors are critical in mechanical and cold pain perception [31]. In addition, we showed above that Cx36 blockade alleviated pT-ION-induced cold allodynia more than mechanical allodynia. Therefore, we hypothesized that Cx36 expressed in the Nav1.8-expressing nociceptors of the TG contributes to pT-ION-induced cold allodynia. To this end, we first tested the changes of Cx36 expression in Nav1.8-positive neurons. Immunofluorescence staining showed that Cx36 was expressed in Nav1.8-positive neurons, and the

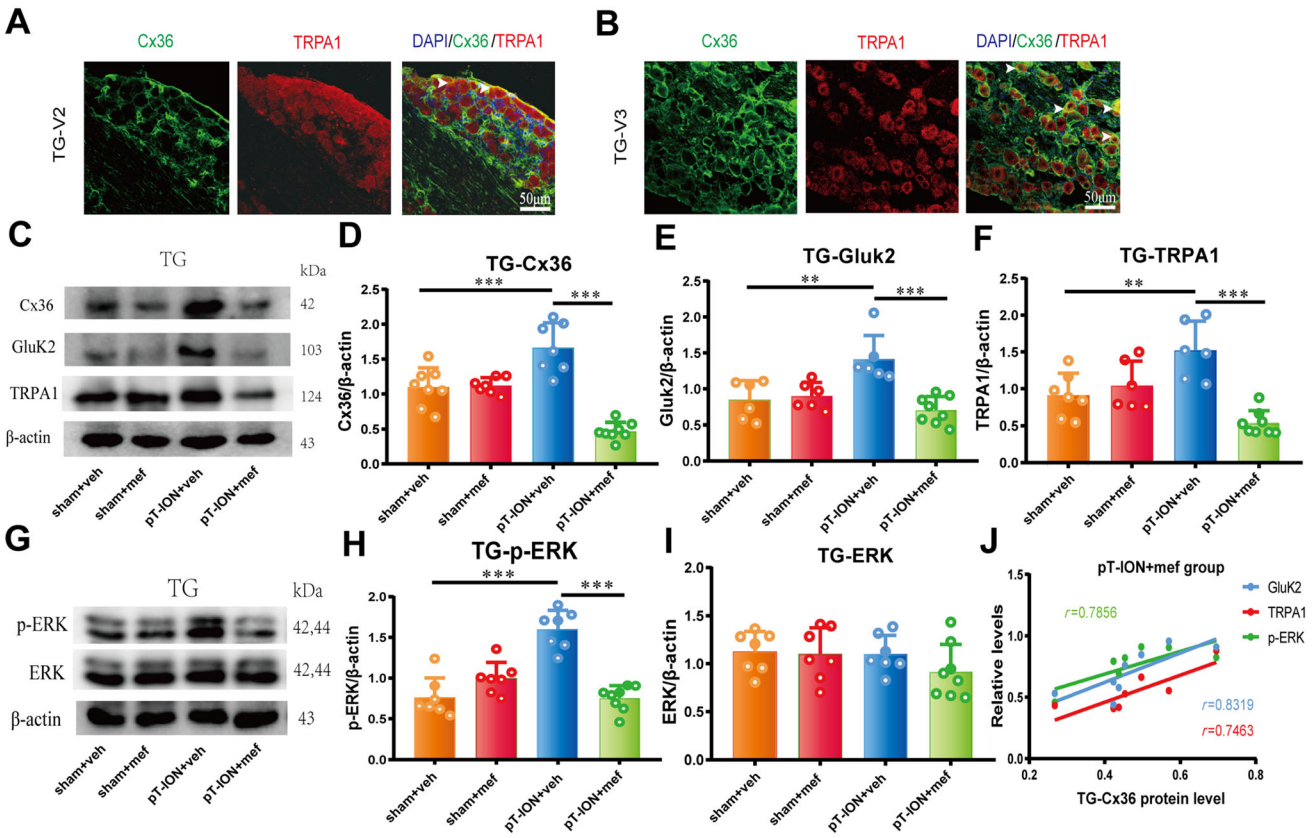

Fig. 5 The Cx36 inhibitor mefloquine reverses the pT-ION-induced increase in expression of Cx36, GluK2, TRPA1, and p-ERK. **A**, **B** Cx36 (green) is co-localized with TRPA1 (red) in both the TG-V2 (**A**) and TG-V3 (**B**) in pT-ION mice (scale bars, 50 μm). DAPI was used to stain the cell nuclei. **C–I** The pT-ION–induced upregulation of Cx36, GluK2, TRPA1, and p-ERK in the ipsilateral TG is reversed by repeated application of the Cx36 inhibitor mefloquine (mef, 20 mg/kg, *i.p.*, once a day from day 7 to day 13 after pT-ION). Data are shown as means ± SEM, n = 7/group. $^{**}P < 0.01$ and $^{***}P < 0.001$ (one-way ANOVA followed by Tukey's test). **J** The decrease in GluK2, TRPA1, and p-ERK expression by the Cx36 inhibitor mefloquine (20 mg/kg, *i.p.*) is positively correlated with the mefloquine-induced downregulation of Cx36 (GluK2-Cx36: $P = 0.0208$, $r = 0.7856$; TRPA1-Cx36: $P = 0.0104$, $r = 0.8319$; p-ERK-Cx36: $P = 0.0334$; $r = 0.7463$).

expression was significantly increased after pT-ION compared with the sham group (Fig. S4). The expression of GluK2 showed similar results. We then subcutaneously injected Cre-dependent AAV-Cx36-Int or AAV-control virus into Nav1.8-Cre mice to selectively knock down Cx36 expression in Nav1.8-expressing nociceptors. The virus was injected at four sites in the orofacial area with 2 μL of virus in each site (Fig. 7A). This viral vector is retrogradely transported from the nerve endings into the somata of TG neurons to interfere with the expression of Cx36. The pT-ION surgery was performed immediately after virus injection in Nav1.8-Cre mice, and the virus was allowed 3 weeks to reach peak infection. As is indicated in Fig. 7D, the AAV-Cx36-Int virus, but not the AAV-control virus, completely reversed the pT-ION-induced cold allodynia in the V3 area, which started at day 21 after virus injection (the infection peak) and lasted for at least 7 days. However, no distinct alleviation of mechanical allodynia in the V2 or V3 regions was found (Fig. 7B, C). Western blotting was used to explore the changes in Cx36 and the downstream molecules in TG samples on day 28 after virus injection. The AAV-Cx36-Int virus reversed the pT-ION-induced upregulation of Cx36, GluK2, TRPA1, and p-ERK, but no significant difference was found for total ERK expression (Fig. 7E–K). The downregulation of GluK2, TRPA1, and p-ERK was positively correlated with the downregulation of Cx36 in the AAV-Cx36-Int virus group (GluK2-Cx36: $P = 0.0093$, $r = 0.8387$, $Y = 0.8486 * X + 0.1443$; TRPA1-Cx36: $P = 0.0312$, $r = 0.7526$, $Y = 1.131 * X + 0.03634$; p-ERK-Cx36: $P = 0.0409$, $r = 0.7272$, $Y = 0.6553 * X + 0.2932$; Fig. 7L). Furthermore, immunofluorescence staining also showed the downregulation of Cx36 in Nav1.8-positive neurons (Fig. S5). These results support our hypothesis that Cx36 and the downstream pathway in Nav1.8-expressing nociceptors only contribute to the pT-ION-induced cold allodynia.

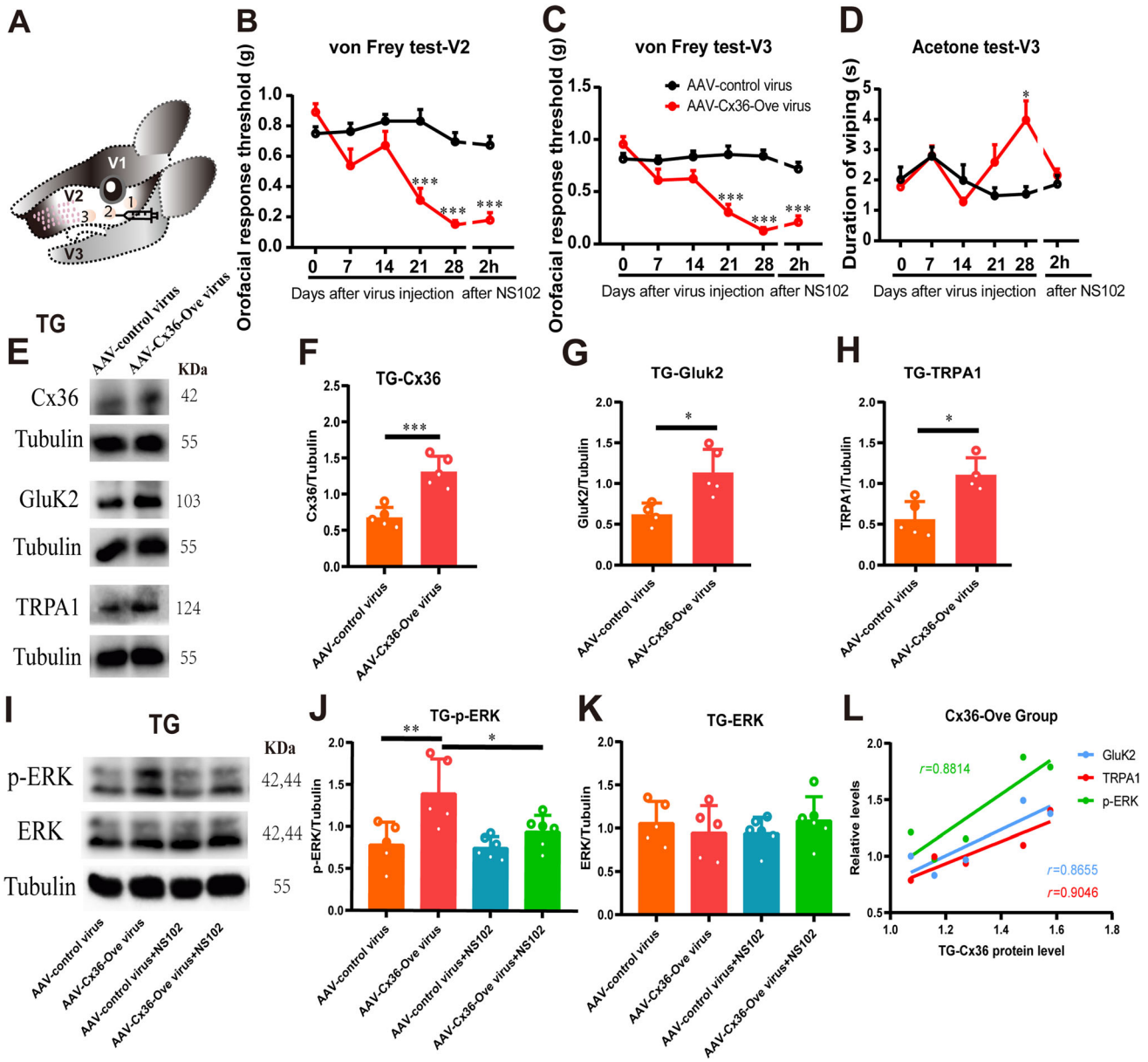

Fig. 6 The orofacial allodynia and the upregulation of GluK2 and TRPA1 induced by Cx36 overexpression in TG-V2 neurons and the effects of the GluK2 antagonist NS 102. **A** Schematic of the three injection sites in the V2 skin area. **B–D** Cx36 overexpression in TG-V2 neurons induces mechanical allodynia in both the V2 (**B**) and V3 (**C**) skin areas and cold allodynia in the V3 area (**D**). Data are shown as means ± SEM, $n = 10$/group. $^{*}P < 0.05$ and $^{***}P < 0.001$ *vs* AAV-control virus (two-way RM ANOVA followed by Sidak's test). **E–H** The expression of Cx36, GluK2, and TRPA1 increases after Cx36 overexpression. **I–K** The upregulation of p-ERK induced by Cx36 overexpression is reversed by the GluK2 antagonist NS-102. Data are shown as means ± SEM, $n = 5$ for the AAV-control virus group and AAV-Cx36-Ove virus group, $n = 6$ for the AAV-control virus+NS102 group and AAV-Cx36-Ove virus+NS102 group. $^{*}P < 0.05$, $^{**}P < 0.01$, $^{***}P < 0.001$ (one-way ANOVA followed by Tukey's test). **L** The increase in GluK2, TRPA1, and p-ERK expression induced by Cx36 overexpression is positively correlated with the upregulation of Cx36 (GluK2-Cx36: $P = 0.0580$, $r = 0.8655$; TRPA1-Cx36: $P = 0.0349$, $r = 0.9046$; p-ERK-Cx36: $P = 0.0482$; $r = 0.8814$).

Discussion

Trigeminal neuralgia is one of the most intractable diseases of the nervous system, and a lack of understanding of its underlying etiology has limited the development of treatments. Our study demonstrates that pT-ION results in increased expression of Cx36 in the ipsilateral TG and that this upregulation is associated with mechanical and cold allodynia. Blocking Cx36 with mefloquine reversed the pT-ION-induced mechanical and cold allodynia and increased GluK2, TRPA1, and p-ERK expression. In addition, overexpressing Cx36 in TG-V2 neurons induced

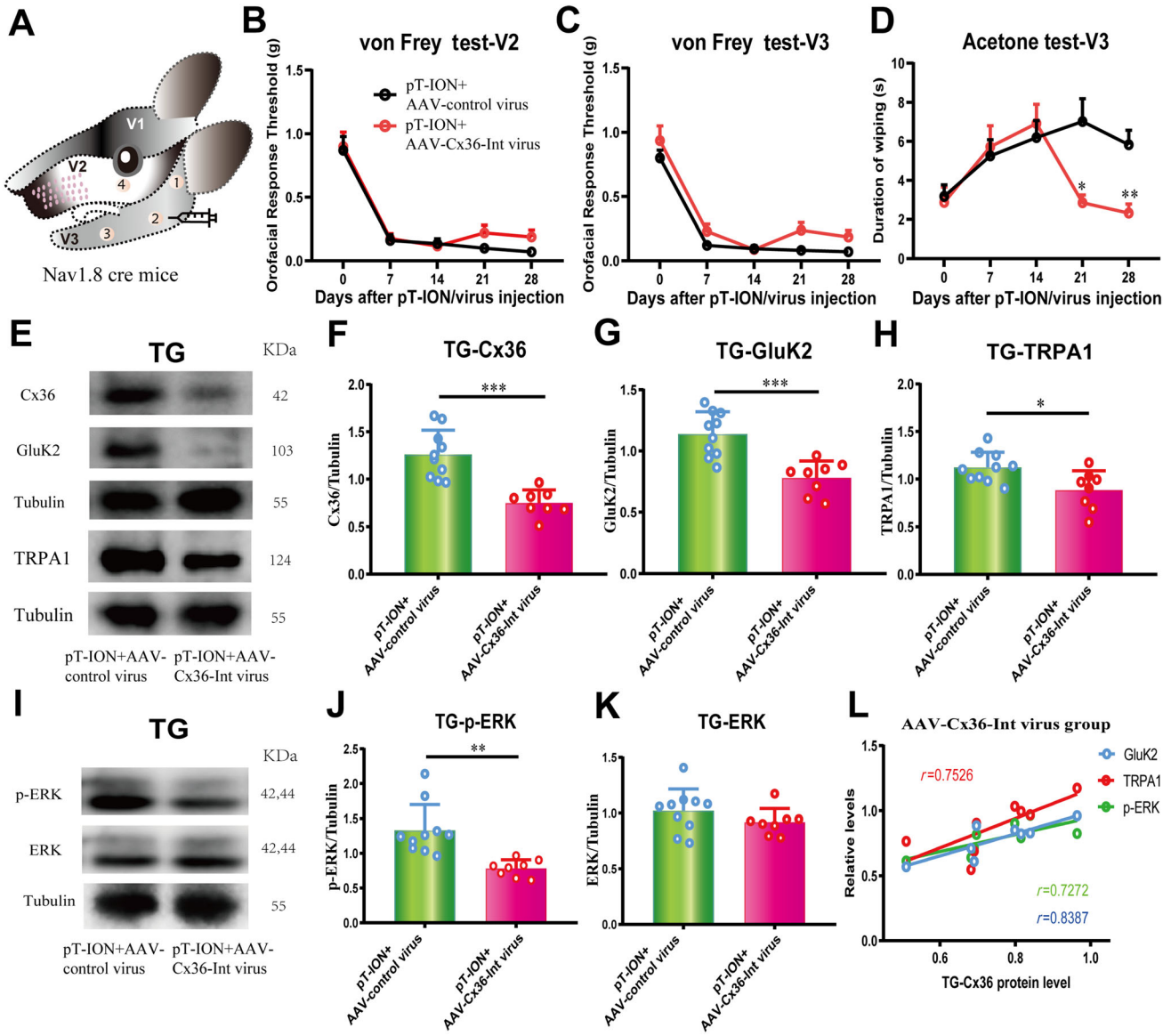

Fig. 7 The reversal of pT-ION-induced cold allodynia and the upregulation of Cx36, GluK2, TRPA1, and p-ERK by genetic inhibition of Cx36 expression in Nav1.8-Cre mice. **A** Schematic of the four injection sites in the V2 and V3 skin areas. **B–D** Cx36 knockdown in TG-V2 and TG-V3 neurons alleviates cold allodynia (**D**) in the V3 skin area but not mechanical allodynia in either the V2 (**B**) or V3 (**C**) areas starting from 21 days after pT-ION (*i.e.* 21 days after virus injection). Data are shown as means ± SEM, $n = 10$/group. $^{*}P < 0.05$ and $^{**}P < 0.01$ *vs* AAV-control virus (two-way RM ANOVA followed by Sidak's test). **E–K** The pT-ION-induced upregulation of GluK2, TRPA1, and p-ERK is reversed by Cx36 knockdown through subcutaneous injection of AAV-Cx36-Int virus at 28 days after pT-ION (*i.e.* 28 days after virus injection). Data are shown as means ± SEM, $n = 7$/group. $^{*}P < 0.05$, $^{**}P < 0.01$, and $^{***}P < 0.001$ (Student's unpaired *t*-test). **L** The AAV-Cx36-Int virus-mediated decrease in GluK2, TRPA1, and p-ERK expression is positively correlated with the downregulation of Cx36 (GluK2-Cx36: $P = 0.0093$, $r = 0.8387$; TRPA1-Cx36: $P = 0.0312$, $r = 0.7526$; p-ERK-Cx36: $P = 0.0409$; $r = 0.7272$).

stable mechanical and cold allodynia in both the V2 and V3 areas, and the cold allodynia but not the mechanical allodynia was reversed by the GluK2 antagonist NS102. Specifically knocking down Cx36 expression in Nav1.8-expressing nociceptors suppressed cold allodynia but did not suppress mechanical allodynia. On the whole, we suggest that Cx36 in the TG mediates orofacial pain hypersensitivity through GluK2 and TRPA1 signaling, and Cx36 in Nav1.8-expressing nociceptors in particular contributes to the induction of orofacial cold allodynia (Fig. 8).

We developed a mouse model of pT-ION that presents with stable primary allodynia in the V2 skin area and secondary allodynia in the V3 skin area. In the pT-ION model we cut off and removed a 1 – 2 mm segment of the distal infraorbital nerve, which causes a more rapid

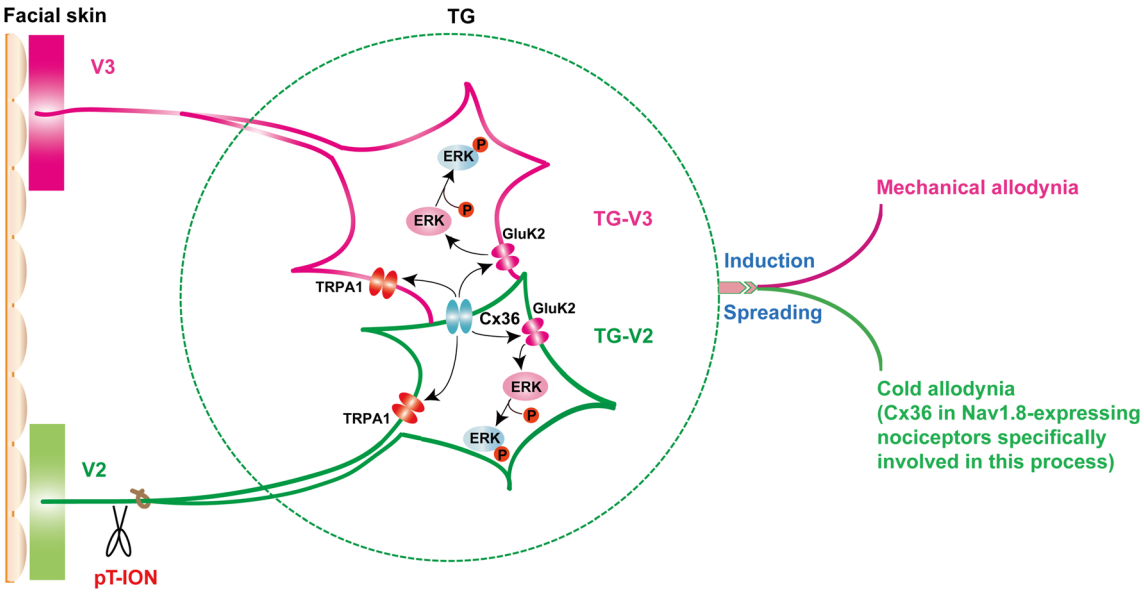

Fig. 8 Schematic of the proposed mechanism. pT-ION induces the upregulation of Cx36 and the downstream activation of GluK2, TRPA1, and ERK, which leads to hyperactivity of primary TG-V2 subdivision neurons. The sensitization of TG-V2 neurons subsequently activates the TG-V3 neurons through Cx36 gap junctions. GluK2, TRPA1, and the downstream ERK are activated in TG-V3 neurons, resulting in the spread of behavioral hypersensitivity to nearby uninjured facial skin. pT-ION, spared nerve injury of the infraorbital nerve; TG, trigeminal ganglion; Cx36, connexin 36; GluK2, kainate receptor.

allodynia onset and stabilization than the traditional model of chronic constriction injury of the infraorbital nerve [32, 33]. The pT-ION model was established by the ligation and removal of the infraorbital nerve, which consists purely of sensory fibers. Consistent with previous reports [27, 34, 35], we found that trigeminal nerve injury leads to both mechanical and cold allodynia. In addition, the increased sensitivity to mechanical stimulation and cold has similarities with the clinical presentation of patients with trigeminal neuralgia [36].

Gap junctions play a critical role in the nervous system, and they have been shown to take part in neurogenesis, differentiation, and information transmission [37, 38]. It has been reported that electrical coupling contributes to the synchronous activation of adjacent neurons after nerve injury [39], which thus provides a new mechanism for the induction of pain hypersensitivity [40]. Several kinds of Cxs are expressed in the TG, including Cx26, which is located between neurons and SGCs, Cx36, which is specifically expressed between neurons, and Cx43, which is expressed between SGCs [26]. Here, we found that secondary orofacial allodynia occurred quite early, starting from 7 days after pT-ION and at almost the same time as primary allodynia. We assume that TG-V2 neurons rapidly activate TG-V3 neurons through gap junctions, and thus secondary allodynia in the V3 area is quickly induced. Spreading is quite common in persistent pain and is commonly considered to be associated with CNS activity [33], but our present work provides a possible peripheral mechanism mediated by gap junctions. It has been reported that increased expression of Cx36 in the medullary dorsal horn contributes to trigeminal nerve injury-induced mechanical allodynia by coupling GABA cells [24]. We found that the expression of Cx36 was upregulated in the TG after nerve injury, but there are no GABA cells in the TG, so whether and how Cx36 in the TG is involved in the development of orofacial pain hypersensitivity is unknown.

We found that mefloquine, which is widely used to prevent malaria and acts as a specific Cx36 inhibitor [41], reduced chronic neuropathic pain and both primary and secondary allodynia. It should be noted that the cold allodynia was reversed immediately after the repeated injection of mefloquine for 7 consecutive days, while the alleviation of mechanical allodynia occurred 7 days after the last injection. This might be due to the cumulative effects of repeated injection of mefloquine, and the progressive suppression of TRPA1 or other unknown protein expression to a low level at 7 days after the last injection might lie behind the delayed alleviation of the mechanical allodynia. We found that repeated injection of mefloquine led to the downregulation of Cx36 in the TG and the alleviation of orofacial pain, which is consistent with a previous report that knocking down Cx36 expression in the anterior cingulate cortex (ACC) by RNA interference alleviates neuropathic pain [41]. Meanwhile, it should be noted that the effects of mefloquine on the ACC or other central nuclei cannot be excluded because of mefloquine's ability to across the blood-brain barrier. However, in the

present study, the AAV-mediated Cx36 overexpression in the TG induced both mechanical and cold allodynia and thus strongly supports a significant contribution of Cx36 in the TG to the development of orofacial pain hypersensitivity. The low dose (20 mg/kg, *i.p.*) and high dose (30 mg/kg, *i.p.*) had similar effects in attenuating chronic neuropathic pain, but some mice in the high-dosage group demonstrated numbness and lethargy, which was not found in the low-dose group. Mefloquine has been reported to be a safe and effective antimalarial drug [42], but we assume that the numbness and lethargy are side-effects of mefloquine, and further pharmacological studies are needed to test this.

Subcutaneous AAV-Cx36-Int virus and AAV-Cx36-Ove virus injection in the V2 or V3 skin, which selectively targeted TG neurons, was a good tool for separately investigating the mechanisms of primary and secondary allodynia and allowed the model to be duplicated in the V2 and V3 area. We found that cold allodynia in the V3 area was induced upon acetone stimulation after pT-ION, which was consistent with previous reports [27, 34]. Also, we found that trigeminal nerve injury induced pain-like behaviors in mice, which was consistent with the pain and the highly sensitive cold sensation in patients suffering from trigeminal neuralgia [36]. The AAVs used in this study were subcutaneously delivered to infect TG neurons. At present, AAV is the only viral vector used in clinical research, and optimizing its mode of administration provides a useful approach that can be used for gene therapy for pain in humans.

In the present study, GluK2 was found to be widely expressed and to co-localize with Cx36, and GluK2 expression was increased in the TG after pT-ION. GluK2, which is a novel cold sensor [29], is more sensitive to temperature than TRPA1 and TRPV1. Also, as a subtype of kainate receptors, GluK2 has been shown to take part in both excitatory and inhibitory neurotransmission and to contribute to the development of synaptic plasticity [43]. Here, GluK2 was found to act downstream of Cx36 and to play a key role in mediating the cold allodynia induced either by trigeminal nerve injury or by Cx36 overexpression. Patients with trigeminal neuralgia are usually sensitive to cold stimulation such as a cold wind and cold water. The finding that GluK2 blockade significantly alleviated nerve injury-induced cold allodynia provides a GluK2-targeting approach for treating trigeminal neuralgia. However, until now there have been no reports of its involvement in allodynia induced by mechanical stimulation. Also, the present work does not support a potential contribution of GluK2 activation to the induction of pT-ION-induced mechanical allodynia. TRPA1 is reported to be located in nociception-specific neurons, and it has been proposed to mediate both mechanical allodynia and cold allodynia [44–47]. Thus, we conclude that GluK2 specifically participates in cold allodynia and plays a role only as a cold sensor, rather than both a mechanical and cold sensor, and that activation of TRPA1 underlies the induction of mechanical allodynia upon Cx36 activation.

ERK belongs to a subfamily of the mitogen-activated protein kinases, and it plays a key role in transmitting extracellular signals to the nucleus [48]. It has been shown that ERK plays an important role in the process of peripheral allodynia and hypersensitivity after harmful stimulation [49, 50]. ERK is activated upon by being phosphorylated and then crosses the nuclear membrane to induce changes in the expression of specific proteins [30, 51, 52]. p-ERK occurs in dorsal root ganglion neurons and the trigeminal spinal nucleus caudalis in inflammatory pain [53, 54]. Our results showed that pT-ION induced an increase in p-ERK expression, which is consistent with a previous study showing that the activation of ERK mediates the development of neuropathic pain [55]. The Cx36 inhibitor mefloquine and the GluK2 antagonist NS 102 reversed the pT-ION-induced upregulation of p-ERK, and this may underlie the analgesic effects of the blockade of Cx36 or GluK2.

The Nav1.8 Na^+ channel is considered to be specifically expressed in nociceptive neurons of medium and small diameters [56]. Nav1.8 is the dominant Na^+ channel in the DRG of mice, and it is speculated to play a similar role in the TG [57]. *SCN10A* is the gene encoding the Nav1.8 channel, and gain-of-function mutations of *SCN10A* have been reported to induce peripheral neuropathic pain [58]. Also, pharmacological knockout of Nav1.8 in mice leads to a total lack of response to harmful mechanical and cold stimulation [31]. Although the role of Nav1.8 in inflammatory pain hypersensitivity seems to be limited, research into neuropathic pain suggests that it is critical for the induction of cold allodynia and not mechanical allodynia [59, 60]. Therefore, the nociceptors expressing Nav1.8 play a critical role in the induction and modulation of noxious and cold hypersensitivity in neuropathic pain. The mouse model of pT-ION is a typical trigeminal neuropathic pain model, and the present work found that specifically knocking down Cx36 in Nav1.8-expressing nociceptors only alleviated pT-ION-induced cold allodynia and not mechanical pain. Thus, we assume that activation of Cx36 and the downstream GluK2 may contribute to cold allodynia by changing the activity of Nav1.8-expressing nociceptors. It should be noted that TRPA1 expression was also decreased in the AAV-Cx36-Int virus group; however, the mechanical allodynia was not significantly alleviated. This is might be because the decrease in TRPA1 expression was only slight and thus was not sufficient to rescue the decreased threshold in response to mechanical stimulation. The other hypothesis is that TRPA1 in Nav1.8-positive

neurons of the TG is predominantly involved in the induction of pT-ION-induced cold allodynia, while TRPA1 in Nav1.8-negative neurons might strongly contribute to the induction of pT-ION-induced mechanical allodynia.

In conclusion, our findings suggest that pT-ION surgery induces upregulation of Cx36 in the ipsilateral TG, which promotes the occurrence of mechanical and cold allodynia in both the V2 and V3 areas through the action of GluK2, TRPA1, and p-ERK as downstream proteins. Our results also indicate the potential of Cx36, GluK2, or TRPA1 antagonists in treating trigeminal neuralgia in clinical practice, which should be the focus of future studies.

Acknowledgements This work was supported by the National Natural Science Foundation of China (81971056, 31600852, 81771202, and 81873101), the Innovative Research Team of High-level Local Universities in Shanghai, the Foundation of Science, Technology and Innovation Commission of Shenzhen Municipality (JCYJ20180302153701406), the National Key R&D Program of China (2017YFB0403803), the Shanghai Municipal Science and Technology Major Project (2018SHZDZX01), and ZJLab.

Conflict of interest All authors claim that there are no conflicts of interest.

References

1. Imbe H, Iwata K, Zhou QQ, Zou S, Dubner R, Ren K. Orofacial deep and cutaneous tissue inflammation and trigeminal neuronal activation. Implications for persistent temporomandibular pain. Cells Tissues Organs 2001, 169: 238–247.
2. Zakrzewska JM, Wu J, Mon-Williams M, Phillips N, Pavitt SH. Evaluating the impact of trigeminal neuralgia. Pain 2017, 158: 1166–1174.
3. Sugiyama T, Shinoda M, Watase T, Honda K, Ito R, Kaji K, *et al.* Nitric oxide signaling contributes to ectopic orofacial neuropathic pain. J Dent Res 2013, 92: 1113–1117.
4. Campbell JN, Meyer RA. Mechanisms of neuropathic pain. Neuron 2006, 52: 77–92.
5. Kim YS, Chu Y, Han L, Li M, Li Z, LaVinka PC, *et al.* Central terminal sensitization of TRPV1 by descending serotonergic facilitation modulates chronic pain. Neuron 2014, 81: 873–887.
6. Shinoda M, Iwata K. Neural communication in the trigeminal ganglion contributes to ectopic orofacial pain. J Oral Biosci 2013, 55: 165–168.
7. Jeon YH, Youn DH. Spinal gap junction channels in neuropathic pain. Korean J Pain 2015, 28: 231–235.
8. Goldberg GS, Lampe PD, Nicholson BJ. Selective transfer of endogenous metabolites through gap junctions composed of different connexins. Nat Cell Biol 1999, 1: 457–459.
9. Devor M, Amir R, Rappaport ZH. Pathophysiology of trigeminal neuralgia: the ignition hypothesis. Clin J Pain 2002, 18: 4–13.
10. Rappaport ZH, Devor M. Trigeminal neuralgia: the role of self-sustaining discharge in the trigeminal ganglion. Pain 1994, 56: 127–138.
11. Spray DC, Hanani M. Gap junctions, pannexins and pain. Neurosci Lett 2019, 695: 46–52.
12. Chen MJ, Kress B, Han X, Moll K, Peng W, Ji RR, *et al.* Astrocytic CX43 hemichannels and gap junctions play a crucial role in development of chronic neuropathic pain following spinal cord injury. Glia 2012, 60: 1660–1670.
13. Kang J, Kang N, Lovatt D, Torres A, Zhao Z, Lin J, *et al.* Connexin 43 hemichannels are permeable to ATP. J Neurosci 2008, 28: 4702–4711.
14. Vit JP, Jasmin L, Bhargava A, Ohara PT. Satellite glial cells in the trigeminal ganglion as a determinant of orofacial neuropathic pain. Neuron Glia Biol 2006, 2: 247–257.
15. Pannese E, Ledda M, Cherkas PS, Huang TY, Hanani M. Satellite cell reactions to axon injury of sensory ganglion neurons: increase in number of gap junctions and formation of bridges connecting previously separate perineuronal sheaths. Anat Embryol (Berl) 2003, 206: 337–347.
16. Chen G, Park CK, Xie RG, Berta T, Nedergaard M, Ji RR. Connexin-43 induces chemokine release from spinal cord astrocytes to maintain late-phase neuropathic pain in mice. Brain 2014, 137: 2193–2209.
17. Ohara PT, Vit JP, Bhargava A, Jasmin L. Evidence for a role of connexin 43 in trigeminal pain using RNA interference in vivo. J Neurophysiol 2008, 100: 3064–3073.
18. Kaji K, Shinoda M, Honda K, Unno S, Shimizu N, Iwata K. Connexin 43 contributes to ectopic orofacial pain following inferior alveolar nerve injury. Mol Pain 2016, 12.
19. Spray DC, Iglesias R, Shraer N, Suadicani SO, Belzer V, Hanstein R, *et al.* Gap junction mediated signaling between satellite glia and neurons in trigeminal ganglia. Glia 2019, 67: 791–801.
20. Niederberger E, Kuhlein H, Geisslinger G. Update on the pathobiology of neuropathic pain. Expert Rev Proteomics 2008, 5: 799–818.
21. Rash JE, Yasumura T, Dudek FE, Nagy JI. Cell-specific expression of connexins and evidence of restricted gap junctional coupling between glial cells and between neurons. J Neurosci 2001, 21: 1983–2000.
22. Long MA, Deans MR, Paul DL, Connors BW. Rhythmicity without synchrony in the electrically uncoupled inferior olive. J Neurosci 2002, 22: 10898–10905.
23. Deans MR, Gibson JR, Sellitto C, Connors BW, Paul DL. Synchronous activity of inhibitory networks in neocortex requires electrical synapses containing connexin36. Neuron 2001, 31: 477–485.
24. Ouachikh O, Hafidi A, Boucher Y, Dieb W. Electrical synapses are involved in orofacial neuropathic pain. Neuroscience 2018, 382: 69–79.
25. Nagy JI, Lynn BD, Senecal JMM, Stecina K. Connexin36 expression in primary afferent neurons in relation to the axon reflex and modality coding of somatic sensation. Neuroscience 2018, 383: 216–234.
26. Garrett FG, Durham PL. Differential expression of connexins in trigeminal ganglion neurons and satellite glial cells in response to chronic or acute joint inflammation. Neuron Glia Biol 2008, 4: 295–306.
27. Cui WQ, Chu YX, Xu F, Chen T, Gao L, Feng Y, *et al.* Calcium channel alpha2delta1 subunit mediates secondary orofacial hyperalgesia through PKC-TRPA1/gap junction signaling. J Pain 2020, 21: 238–257.
28. Seemann N, Welling A, Rustenbeck I. The inhibitor of connexin Cx36 channels, mefloquine, inhibits voltage-dependent Ca(2+) channels and insulin secretion. Mol Cell Endocrinol 2018, 472: 97–106.
29. Gong J, Liu J, Ronan EA, He F, Cai W, Fatima M, *et al.* A cold-sensing receptor encoded by a glutamate receptor gene. Cell 2019, 178: 1375–1386.e1311.
30. Ji RR, Gereau RWT, Malcangio M, Strichartz GR. MAP kinase and pain. Brain Res Rev 2009, 60: 135–148.

31. Abrahamsen B, Zhao J, Asante CO, Cendan CM, Marsh S, Martinez-Barbera JP, *et al.* The cell and molecular basis of mechanical, cold, and inflammatory pain. Science 2008, 321: 702–705.
32. Imamura Y, Kawamoto H, Nakanishi O. Characterization of heat-hyperalgesia in an experimental trigeminal neuropathy in rats. Exp Brain Res 1997, 116: 97–103.
33. Ringkamp M, Meyer RA. Injured versus uninjured afferents: Who is to blame for neuropathic pain? Anesthesiology 2005, 103: 221–223.
34. Lim EJ, Jeon HJ, Yang GY, Lee MK, Ju JS, Han SR, *et al.* Intracisternal administration of mitogen-activated protein kinase inhibitors reduced mechanical allodynia following chronic constriction injury of infraorbital nerve in rats. Prog Neuropsychopharmacol Biol Psychiatry 2007, 31: 1322–1329.
35. Guo QH, Tong QH, Lu N, Cao H, Yang L, Zhang YQ. Proteomic analysis of the hippocampus in mouse models of trigeminal neuralgia and inescapable shock-induced depression. Neurosci Bull 2018, 34: 74–84.
36. Scrivani S, Wallin D, Moulton EA, Cole S, Wasan AD, Lockerman L, *et al.* A fMRI evaluation of lamotrigine for the treatment of trigeminal neuropathic pain: pilot study. Pain Med 2010, 11: 920–941.
37. Eugenin EA, Basilio D, Saez JC, Orellana JA, Raine CS, Bukauskas F, *et al.* The role of gap junction channels during physiologic and pathologic conditions of the human central nervous system. J Neuroimmune Pharmacol 2012, 7: 499–518.
38. Akbarpour B, Sayyah M, Babapour V, Mahdian R, Beheshti S, Kamyab AR. Expression of connexin 30 and connexin 32 in hippocampus of rat during epileptogenesis in a kindling model of epilepsy. Neurosci Bull 2012, 28: 729–736.
39. Kim YS, Anderson M, Park K, Zheng Q, Agarwal A, Gong C, *et al.* Coupled activation of primary sensory neurons contributes to chronic pain. Neuron 2016, 91: 1085–1096.
40. Devor M, Wall PD. Cross-excitation in dorsal root ganglia of nerve-injured and intact rats. J Neurophysiol 1990, 64: 1733–1746.
41. Chen ZY, Shen FY, Jiang L, Zhao X, Shen XL, Zhong W, *et al.* Attenuation of neuropathic pain by inhibiting electrical synapses in the anterior cingulate cortex. Anesthesiology 2016, 124: 169–183.
42. Tine RC, Faye B, Sylla K, Ndiaye JL, Ndiaye M, Sow D, *et al.* Efficacy and tolerability of a new formulation of artesunate-mefloquine for the treatment of uncomplicated malaria in adult in Senegal: open randomized trial. Malar J 2012, 11: 416.
43. Evans AJ, Gurung S, Henley JM, Nakamura Y, Wilkinson KA. Exciting times: New advances towards understanding the regulation and roles of kainate receptors. Neurochem Res 2019, 44: 572–584.
44. Kwan KY, Allchorne AJ, Vollrath MA, Christensen AP, Zhang DS, Woolf CJ, *et al.* TRPA1 contributes to cold, mechanical, and chemical nociception but is not essential for hair-cell transduction. Neuron 2006, 50: 277–289.
45. Obata K, Katsura H, Mizushima T, Yamanaka H, Kobayashi K, Dai Y, *et al.* TRPA1 induced in sensory neurons contributes to cold hyperalgesia after inflammation and nerve injury. J Clin Invest 2005, 115: 2393–2401.
46. Trevisan G, Benemei S, Materazzi S, De Logu F, De Siena G, Fusi C, *et al.* TRPA1 mediates trigeminal neuropathic pain in mice downstream of monocytes/macrophages and oxidative stress. Brain 2016, 139: 1361–1377.
47. Moore C, Gupta R, Jordt SE, Chen Y, Liedtke WB. Regulation of pain and itch by TRP channels. Neurosci Bull 2018, 34: 120–142.
48. Lin MW, Lin CC, Chen YH, Yang HB, Hung SY. Celastrol inhibits dopaminergic neuronal death of Parkinson's disease through activating mitophagy. Antioxidants (Basel) 2019, 9: 37. https://doi.org/10.3390/antiox9010037.
49. Zhuang ZY, Xu H, Clapham DE, Ji RR. Phosphatidylinositol 3-kinase activates ERK in primary sensory neurons and mediates inflammatory heat hyperalgesia through TRPV1 sensitization. J Neurosci 2004, 24: 8300–8309.
50. Dai Y, Iwata K, Fukuoka T, Kondo E, Tokunaga A, Yamanaka H, *et al.* Phosphorylation of extracellular signal-regulated kinase in primary afferent neurons by noxious stimuli and its involvement in peripheral sensitization. J Neurosci 2002, 22: 7737–7745.
51. Impey S, Obrietan K, Storm DR. Making new connections: role of ERK/MAP kinase signaling in neuronal plasticity. Neuron 1999, 23: 11–14.
52. Cao H, Ren WH, Zhu MY, Zhao ZQ, Zhang YQ. Activation of glycine site and GluN2B subunit of NMDA receptors is necessary for ERK/CREB signaling cascade in rostral anterior cingulate cortex in rats: implications for affective pain. Neurosci Bull 2012, 28: 77–87.
53. Noma N, Tsuboi Y, Kondo M, Matsumoto M, Sessle BJ, Kitagawa J, *et al.* Organization of pERK-immunoreactive cells in trigeminal spinal nucleus caudalis and upper cervical cord following capsaicin injection into oral and craniofacial regions in rats. J Comp Neurol 2008, 507: 1428–1440.
54. Ji RR, Befort K, Brenner GJ, Woolf CJ. ERK MAP kinase activation in superficial spinal cord neurons induces prodynorphin and NK-1 upregulation and contributes to persistent inflammatory pain hypersensitivity. J Neurosci 2002, 22: 478–485.
55. Shao S, Xia H, Hu M, Chen C, Fu J, Shi G, *et al.* Isotalatizidine, a C19-diterpenoid alkaloid, attenuates chronic neuropathic pain through stimulating ERK/CREB signaling pathway-mediated microglial dynorphin A expression. J Neuroinflammation 2020, 17: 13.
56. Han C, Huang J, Waxman SG. Sodium channel Nav1.8: emerging links to human disease. Neurology 2016, 86: 473–483.
57. Chang W, Berta T, Kim YH, Lee S, Lee SY, Ji RR. Expression and role of voltage-gated sodium channels in human dorsal root ganglion neurons with special focus on nav1.7, species differences, and regulation by paclitaxel. Neurosci Bull 2018, 34: 4–12.
58. Faber CG, Lauria G, Merkies IS, Cheng X, Han C, Ahn HS, *et al.* Gain-of-function Nav1.8 mutations in painful neuropathy. Proc Natl Acad Sci U S A 2012, 109: 19444–19449.
59. Leo S, D'Hooge R, Meert T. Exploring the role of nociceptor-specific sodium channels in pain transmission using Nav18 and Nav19 knockout mice. Behav Brain Res 2010, 208: 149–157.
60. Foulkes T, Wood JN. Mechanisms of cold pain. Channels (Austin) 2007, 1: 154–160.